Table 3 Inhibition of infection of primate cells by anti-CD4 mAbs

Species	Replication of HIV-1 in the presence of Leu3a	F101-5	MT151	No mAb
Man	−	−	−	++
Owl monkey	−	−	+	++
Red-bellied tamarin	−	−	+	++
Golden lion marmoset	−	++	++	++
White-nosed saki	−	++	++	++

250 μl suspension containing 10^5 PBL in RPMI 1640 with FCS (20%) and IL-2 (100 U) were incubated with 10^5 infections units of HIV-1 in the presence of 20 μg ml^{-1} Leu3a, F101-5 or MT151, or without mAb. One week after infection the cells were washed and co-cultivated with an equal volume and number of C8166 cells. Syncytial formation was evaluated at 24 h. Where many syncytia were observed, as in the control without mAb, this was represented as ++, a significant reduction (<10) was scored as +, and − indicated total absence of syncytia.

well represented on New World monkey PBL. This mAb showed partial inhibition of two species (owl monkey and red-bellied tamarin) that were negative by FACS. This partial blocking of HIV-1 could arise from the high concentration of mAb used (20 μg ml^{-1}, when 1 μg ml^{-1} is sufficient to block HIV-1 infection of human cells), as there may be a low-affinity interaction with CD4 not detected by immunofluorescence.

The mAbs used here have been categorized into two main groups, according to whether or not they blocked the binding of HIV-1 and HIV-2 to human T cells[5,6]. In addition, by cross-competition assays using ^{125}I-labelled antibody, clusters of mAbs were defined which were either wholly distinct from one another, or which competed for the same epitope[5]. Using this panel of characterized mAbs, we have shown that only one CD4 epitope cluster was consistently present in all primate species tested; the mAbs in this cluster are in competition and are therefore directed against the same or overlapping epitopes. Furthermore, HIV-1, HIV-2 and the T-cell tropic simian immunodeficiency viruses SIV_{MAC}, SIV_{MAN} and SIV_{AGM} all use the CD4 receptor on human cells and are blocked by these mAbs (ref. 6), emphasizing the importance of this epitope cluster to HIV/SIV binding. Anti-idiotypic antibodies to Leu3a, a mAb recognizing this epitope, neutralize HIV-1 (refs 8, 9).

Phylogenesis has been considered in relation to T-antigen expression on PBL using anti-CD3, CD4 and CD8 mAbs (refs 10–12), and our study of CD4 extends this analysis. Our findings differ, however, from an earlier report[11] which used a panel of 9 anti-CD4 mAbs and found that the gorilla shared fewer epitopes with man than did two of the three macaques phenotyped (*Macaca mulatta* and *Macaca arctoides*). The conserved epitope cluster recognized by HIVs and SIVs is probably important in the natural function of CD4 in the immune system and other tissues.

Transfer and ectopic expression of the human CD4 gene in human cells renders those cells susceptible to HIV infection, whereas CD4 gene transfer to mouse cells confers sensitivity to HIV binding but not to infection[13]. We have shown that primate CD4 is a receptor for HIV, so the function of human CD4 expressed in cells more closely related to man than mouse is of interest. PBL from several primate species have been infected *in vitro*[14] and *in vivo*[15–18] with simian lentiviruses. SIV_{MAC} (formerly $STLV\text{-}III_{MAC}$) isolated from sick rhesus macaques[15], and SIV_{MAN} from the healthy sooty mangabey[18], have properties similar to HIV and produce an AIDS-like disease in recipient macaques. *In vitro* studies show that SIV_{MAC} replicates efficiently in host macaque PBL and progressively less so in PBL of human, gibbon, ape and baboon, and not at all in PBL from the chimpanzee, the squirrel monkey or the cotton-top tamarin[14]. Also, some simian cells are permissive to replication of HIV-1 and transfer of the cloned proviral genome[19–21].

We have shown that a much wider host range exists than formerly supposed for the infection of non-human primate *in vitro* PBL by HIV-1 and HIV-2, although human cells were more permissive to viral replication than monkey cells. Following HIV-1 inoculation *in vivo*, chimpanzees show seroconversion, transient depression of CD4 lymphocytes, and lymphadenopathy (in one animal), but have not developed AIDS to date[22–24]. In a recent attempt to infect rhesus macaques with HIV-2, three out of eight animals seroconverted within 12 months, but have shown no symptoms of disease so far[25].

We are grateful to C. Mulder, J. N. Weber and C. Hetherington for advice and discussions, to R. S. Tedder for providing us with anti-p18 mAb, and to the following for virus isolates: R. C. Gallo (HTLV-IIIB, HTLV-IIIRF); D. Zagury (Z129) and L. Montagnier (LAV-2). The study was supported by the Wellcome Foundation, the Cancer Research Campaign and the Medical Research Council.

Received 17 August; accepted 23 October 1987.

1. Dalgleish, A. G. *et al. Nature* **312,** 763–767 (1984).
2. Klatzmann, D. *et al. Nature* **312,** 767–768 (1984).
3. McDougal, J. S. *et al. Science* **231,** 382–385 (1986).
4. Clavel, F. *et al. Science* **233,** 343–346 (1986).
5. Sattentau, Q. L., Dalgleish, A. G., Weiss, R. A. & Beverley, P. C. L. *Science* **234,** 1120–1123 (1986).
6. Sattentau, Q. J. *Int. Conf. AIDS* **III,** 160 (1987).
7. Weiss, R. A. *et al. Nature* **324,** 572–575 (1986).
8. Chanh, T. C., Dreesman, G. R. & Kennedy, R. C. *Proc. natn. Acad. Sci. U.S.A.* **84,** 3891–3895 (1987).
9. Sattentau, Q. J., Weber, J. N., Weiss, R. A. & Beverley, P. C. L. *Int. Conf. AIDS* **III,** 160 (1987).
10. Letvin, N. L. *et al. Eur. J. Immun.* **13,** 345–347 (1983).
11. Jonker, M. & Nooij, F. J. M. in *Leucocyte Typing* (eds Bernard, A. *et al.*) 373–388 (Springer, Berlin, 1984).
12. Letvin, N. L. in *Leucocyte Typing* (eds Bernard, A. *et al.*) 389–393 (Springer, Berlin, 1984).
13. Maddon, P. *et al. Cell* **47,** 333–348 (1986).
14. Kannagi, M., Yetz, J. M. & Letvin, N. L. *Proc. natn. Acad. Sci. U.S.A.* **82,** 7053–7057 (1985).
15. Letvin, N. L. *et al. Science* **230,** 71–73 (1985).
16. Baskin, G. B. *et al. J. natn. Cancer Inst.* **77,** 127–139 (1986).
17. Fultz, P. N. *et al. Proc. natn. Acad. Sci. U.S.A.* **83,** 5286–5290 (1986).
18. Murphey-Corb, M. *et al. Nature* **321,** 435–437 (1986).
19. Levy, J. A. *et al. Virology* **147,** 441–448 (1985).
20. Levy, J. A., Cheng-Mayer, C., Dina, D. & Luciw, P. A. *Science* **232,** 998–1001 (1986).
21. Adachi, A. *et al. J. Virol.* **59,** 284–291 (1986).
22. Alter, H. J. *et al. Science* **226,** 549–552 (1984).
23. Fultz, P. N. *et al. J. Virol.* **58,** 116–124 (1986).
24. Nara, P. L. *et al. J. Virol.* **61,** 3173–3180 (1987).
25. Fultz, P. N., Switzer, W. M. & Montagnier, L. *Int. Conf. AIDS* **III,** 212 (1987).
26. Napier, J. R. & Napier, P. H. *A Handbook of Living Primates* (Academic, London, New York, 1967).
27. Gallo, R. C. *Science* **224,** 500–503 (1984).
28. Clapham, P. R. *et al. Virology* **158,** 44–51 (1987).
29. Ferns, B., Tedder, R. S. & Weiss, R. A. *J. gen. Virol.* **68,** 1543–1551 (1987).
30. Matlin, K. S., Reggio, H., Helenius, A. & Simons, K. *J. Cell Biol.* **91,** 601–613 (1981).
31. Hoffman, A. D., Banapour, B. & Levy, J. A. *Virology* **147,** 326–335 (1985).

Anti-termination of transcription within the long terminal repeat of HIV-1 by *tat* gene product

Shaw-Yi Kao*, Andrew F. Calman*, Paul A. Luciw† & B. Matija Peterlin*‡

* Howard Hughes Medical Institute, Department of Medicine and Department of Microbiology and Immunology, University of California, San Francisco, California 94143, USA
† Department of Medical Pathology, University of California, Davis, California 95616, USA

Human immunodeficiency virus-1 (HIV-1) gene expression is controlled by cellular transcription factors and by virally encoded *trans*-activation proteins of the HIV-1 *tat* and *art/trs* genes, which are essential for viral replication[1,9–11]. *Tat trans*-activates HIV-1 gene expression by interacting with the *trans*-acting response element (TAR) located within the HIV-1 long terminal repeat (LTR) (ref. 2). In transient expression assays, *tat* mediates its effects largely by increasing the steady-state levels of messenger RNA species that contain the TAR sequence at or near their 5′ ends[2–4], suggesting a function for *tat* either in transcription or in subsequent

‡ To whom correspondence should be addressed.

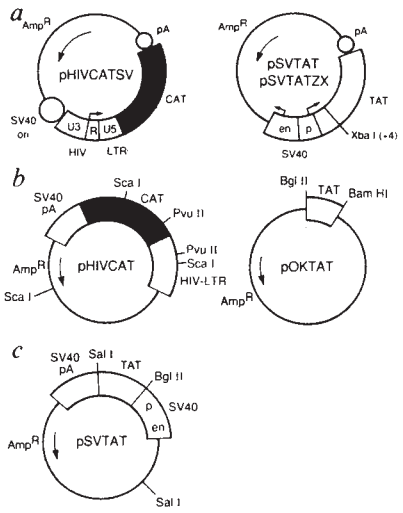

Fig. 1 Plasmids and their restriction sites. *a*, Plasmids used in transient transfection assays. pHIVCATSV contains the HIV-1 LTR linked to the CAT gene. pSVTAT encodes functional *tat*. pSVTATZX, derived from pSVTAT, contains a frameshift mutation which inactivates *tat*. All three plasmids contain the SV40 origin of replication, which permits their replication in COS7 cells. *b*, Plasmids used for Southern blot analysis. pHIVCAT is similar to pHIVCATSV but lacks the SV40 origin of replication. pOKTAT contains the *tat* gene. Other plasmids (not shown): pHIVCATSV2 is similar to pHIVCATSV, except that the SV40 origin of replication is downstream of the CAT gene. pSVΔTAT, derived from pSVTAT, contains a deletion which inactivates *tat*. Key: en, transcriptional enhancer. p, transcriptional promoter. p*A*, polyadenylation site. ori, origin of replication. Large arrows, bacterial ampicillin resistance gene; small arrows, sites and direction of initiation of transcription.

Methods. pHIVCATSV contains 4.5 kilobase (kb) pairs and was constructed by ligation of the 2,200-bp *Eco*RV-*Bam*HI fragment of pHIVCAT (previously designated[3] TAR-1), which contains HIV-1 LTR, CAT and SV40 polyadenylation sequences, into the *Xba*I and *Bam*HI sites of pSVT-2 (ref. 25). pSVTAT (3.8 kb; previously designated TAT-1), which expresses the *tat* protein, has been described[3]. pSVTATZX was derived from pSVTAT by linearizing with *Xba* I (position +21 in *tat*), filling recessed ends, and religating. This introduced four additional nucleotides into the *tat* sequence, creating a frameshift which inactivates *tat*. pOKTAT is a pUC-based plasmid with a few additional restriction sites into which the *tat* gene was cloned. pHIVCATSV2 was derived from pHIVCAT by ligation of a 342-bp fragment containing the SV40 replication origin downstream of the CAT gene. pSVΔTAT was constructed from pSVTAT by deletion of the 83 bp *Xba*I-*Mlu*I fragment in the *tat* gene. All plasmids are based on the vector pML (ref. 26). Structure of all plasmids was verified by restriction mapping and/or DNA sequencing. Production of functional *tat* mRNA from pSVTAT, and of non-functional *tat* mRNA from pSVTATZX and pSVΔTAT, was verified by CAT enzyme assay and *tat* RNA analysis in cotransfected cells (Fig. 2 and data not shown).

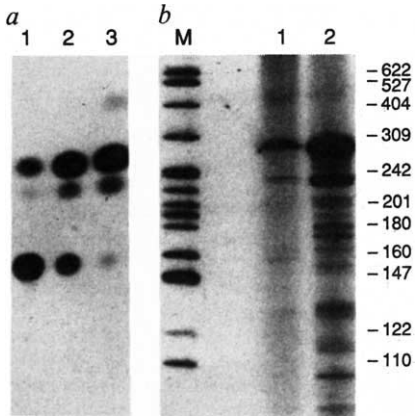

Fig. 2 CAT enzymatic assay and primer extension analysis of cotransfected COS7 cells. COS7 cells were cotransfected with pHIVCATSV and either pSVTATZX or pSVTAT. Cells were collected for CAT enzyme assays and primer extension experiments 48 h later. *a*, CAT enzyme assay of cellular lysates from COS7 cells cotransfected with pHIVCATSV and pSVTATZX (lane 1) or with pHIVCATSV and pSVTAT (lanes 2 and 3). Assays contained 5 μg (lanes 1 and 3) or 1 μg (lane 2) protein from cellular lysates. CAT converts ^{14}C-chloramphenicol to its acetylated forms, which migrate faster on thin layer chromatography plates. *b*, primer extension assay. CAT primer (20 nucleotides, positions +50 to +70 in the CAT gene) was used to prime reverse transcription from 10 μg total RNA from these cotransfected cells. Lane M, molecular weight markers (pBR322 digested with *Msp*I). Fragment sizes (in nucleotides) are indicated at the right. Lane 1, COS7 cells cotransfected with pHIVCATSV and pSVTATZX. Lane 2, COS7 cells cotransfected with pHIVCATSV and pSVTAT. The major band of 280 nucleotides corresponds to transcripts which initiate at the HIV-1 LTR cap site[3].

Methods. COS7 cells were grown in 10-cm tissue culture dishes. Supercoiled plasmid DNA (10 μg) was transfected in 5 ml Dulbecco's modified Eagle medium containing 400 μg ml^{-1} DEAE-dextran, 0.1 mM chloroquine diphosphate and 50 mM Tris-HCl, *p*H 7.5. After a 3 h incubation, cells were washed with serum-free medium and incubated for 48 h in medium containing 10% fetal bovine serum, then scraped from the dishes. A small fraction was lysed by three freeze-thaw cycles for the CAT enzyme assay. RNA was extracted from the remaining cells by the guanidinium isothiocyanate/CsCl method[27]. CAT assays[3] were performed using a 10 min incubation at 37 °C. After thin layer chromatography on silica plates, spots containing monoacetylated and non-acetylated ^{14}C-chloramphenicol were excised and counted by liquid scintillation to determine CAT activity. Primer extensions were performed as described[3], and quantified by scanning densitometry of the autoradiograph.

RNA processing. The *tat* gene could also facilitate translation of mRNA containing the TAR sequence[5–8]. To determine the mechanism of *trans*-activation by *tat*, we analysed the structure and rate of synthesis of RNA species directed by the HIV-1 LTR in transient expression assays both in the presence and absence of *tat*. Although the rate of HIV-1 transcription initiation was not affected by *tat*, transcriptional elongation beyond position +59 was seen only in the presence of *tat*. Thus, *tat trans*-activates HIV-1 transcription by relieving a specific block to transcriptional elongation within the TAR sequence.

In human immunodeficiency viruses, viral gene expression and replication are dependent on virally encoded *trans*-activation proteins[1,9–11]. Infectivity of HIV-1 is abolished by deletions within the gene encoding the viral *trans*-activator *tat*; when *tat* is provided in *trans*, viral gene expression is restored[12] by a mechanism which is not fully understood. We studied the mechanism of HIV-1 *trans*-activation by *tat* in COS7 African green monkey kidney cells. These cells express the T antigen of SV40 and permit efficient replication and expression of plasmids which contain the SV40 origin of replication[13]. We have constructed several such plasmids (Fig. 1). pHIVCATSV contains the HIV-1 LTR linked to the bacterial chloramphenicol acetyltransferase (CAT) reporter gene. pSVTAT (ref. 3) directs the synthesis of functional *tat* protein, whereas pSVTATZX, which contains a frameshift mutation at position +21 of the *tat* gene, encodes a non-functional *tat* protein. pHIVCATSV was cotransfected with either pSVTAT or pSVTATZX into COS7 cells. Using a transient expression assay, we quantified the amounts of steady-state CAT protein and mRNA, measured rates of transcriptional initiation and elongation from the HIV-1 LTR, and mapped HIV-1 transcripts synthesized in the presence and absence of functional *tat*.

Figure 2 shows that when COS7 cells were cotransfected with pHIVCATSV and pSVTATZX, amounts of both CAT enzyme

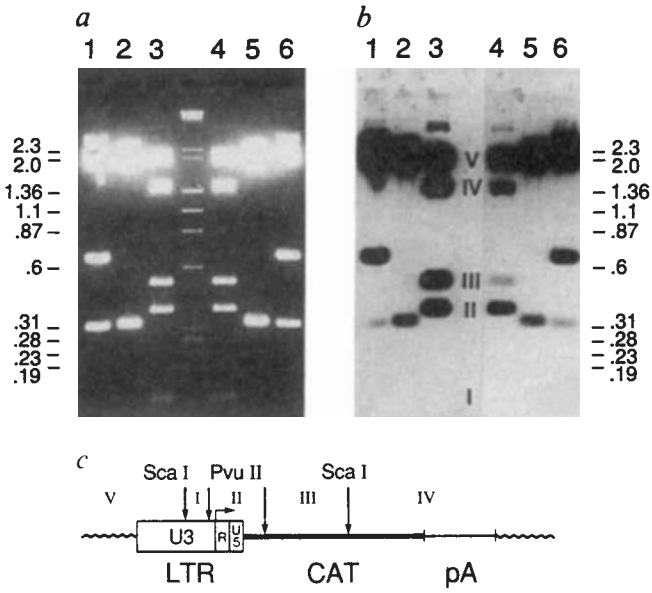

Fig. 3 Nuclear run-on transcription analysis of cotransfected COS7 cells. *a*, Ethidium bromide staining of DNA fragments in a 2% agarose gel used for Southern blotting. Lanes 1 and 6, pSVTAT digested with *Bgl*II and *Sal*I. Lanes 2 and 5, pOKTAT digested with *Bgl*II and *Bam*HI. Lanes 3 and 4, pHIVCAT digested with *Sca*I and *Pvu*II. DNA markers are from bacteriophage λ digested with *Hin*dIII and bacteriophage φX174 digested with *Hae*III; lengths are given in kb. *b*, Hybridization of radiolabelled nascent transcripts to Southern blot of Fig. 3*a*. Lanes 1 to 3, COS7 cells cotransfected with pHIVCATSV and pSVTAT. Lanes 4 to 6, COS7 cells cotransfected with pHIVCATSV and pSVTATZX. Fragments labelled I–V represent restriction fragments of pHIVCAT, as shown in Fig. 3*c*. *c*, Restriction fragments of pHIVCAT digested with *Pvu*II and *Sca*I. Fragment I, 120 bp *Sca*I-*Pvu*II band from the U3 region; fragment II, 360 bp *Pvu*II-*Pvu*II band from the R, U5, and 5′CAT regions; fragment III, 520 bp *Pvu*II-*Sca*I band from the CAT region; fragment IV, 1,400 bp *Sca*I-*Sca*I band from the CAT, SV40 polyA, and pML regions; fragment V, 2,200 bp *Sca*I-*Sca*I band from the pML and U3 regions.

Methods. Restriction digests of 5 μg plasmid DNA were electrophoresed on 2% agarose gels, denatured *in situ* and transferred to nylon membranes (Micron Separations) using 1M ammonium acetate. Because the pSVTAT digest was incomplete, less of the 300 bp *tat* fragment was generated in lanes 1 and 6 than in lanes 2 and 5. The DNA fragments were immobilized on the filters by UV cross-linking, which ensures the retention of small DNA fragments[28]. COS7 cells were cotransfected as in Fig. 2. After a 48 h incubation, the cells were permeabilized with 200 μg ml^{-1} digitonin, and nuclei were incubated with α-^{32}P-UTP for 15 min at 25 °C. RNA was extracted with guanidinium HCl, and 2 × 10^6 c.p.m. RNA was hybridized to each filter for 48 h. Filters were then washed, treated with 10 μg ml^{-1} RNase A for 10 min at 22 °C, and autoradiographed as described[14]. Results were quantified by scanning densitometry of several different exposures of each autoradiograph, normalizing to the *tat* signals. The data shown are representative of five independent experiments. Incorporation of α-^{32}P-UTP was linear from 0–45 min, and an identical pattern of hybridization was obtained using RNA synthesized in either a 5 min or a 15 min reaction.

activity and correctly initiated CAT mRNA were low. In COS7 cells cotransfected with pHIVCATSV and pSVTAT, the concentrations of CAT protein and RNA were increased 40-fold and 33-fold respectively. The extent of *trans*-activation of the HIV-1 LTR by *tat* in COS7 cells was equivalent when similar plasmid constructions which do not contain the SV40 origin of replication were used (data not shown). These results validate the use of replicating plasmids and COS7 cells for the study of HIV-1 *trans*-activation, and confirm and extend our previous analysis of HIV-1 *trans*-activation in human T cells, HeLa cells and Syrian hamster pancreatic cells[3]. Because increases in CAT enzyme activity paralleled the increases in steady-state levels of mRNA transcribed from the HIV-1 LTR, we conclude that *tat* must act at a pretranslational step.

We used an *in vitro* nuclear run-on transcription assay[14] to study the effect of *tat* on the rates of HIV-1 transcriptional initiation and elongation. Radiolabelled nascent transcripts from cotransfected COS7 cells were hybridized to Southern blots of immobilized *tat*, CAT, and HIV-1 LTR sequences (Fig. 1*b* and Fig. 3). Hybridization to the 300-base-pair (bp) *tat* band served as control for both transfection efficiency and total incorporation of radioactive label in each reaction (Fig. 3*b*, lanes 1, 2, 5 and 6).

To compare the transcription rates of different regions of the HIV-1 LTR, pHIVCAT (Fig. 1*b*) was digested with *Sca*I and *Pvu*II (Fig. 3*a*, lanes 3 and 4). These two restriction enzymes yield five DNA fragments representing sequences upstream and downstream from the site of inititiation of HIV-1 transcription (Fig. 3*c*). No hybridization to the HIV-1 LTR U3 region (fragment I) was detected (Fig. 3*b*); thus, little or no transcription occurs from upstream of the cap site. RNA transcribed both in the presence and absence of *tat* hybridized strongly to fragment II, which contains sequences from the R and U5 regions of the HIV-1 1 LTR and the CAT gene (Fig. 3*b* and *c*). In contrast, hybridization to fragment III, which contains only CAT sequences, was 47-fold higher in cells cotransfected with pHIVCATSV and pSVTAT than in cells cotransfected with pHIVCATSV and pSVTATZX. In both samples, equivalent hybridization was observed to pML sequences transcribed from the SV40 late promoter contained in pSVTAT and pSVTATZX (fragments IV and V). We conclude that *tat* does not affect the rate of HIV-1 initiation of transcription, but is required for transcriptional elongation through the HIV-1 LTR. This suggests that only short transcripts are synthesized in the absence of *tat*.

To identify and map these predicted short transcripts, we used an RNase protection assay to analyse the HIV-1 LTR RNA species synthesized in the presence or absence of *tat* (Fig. 4*a*). ^{32}P-labelled HIV-1 LTR anti-sense RNA probes A and B (Fig. 4*b*) were hybridized to RNA from COS7 cells cotransfected with pHIVCATSV2 and either pSVTAT or pSVΔTAT (Fig. 1, legend), digested with RNases A and T1, and analysed by polyacrylamide gel electrophoresis. In the presence of *tat*, the predominant protected band (205 nucleotides with probe A, 185 nucleotides with probe B) corresponded to HIV-1 LTR transcripts which were initiated at position +1 and elongated beyond position +184 (Fig. 4*a*, lanes 2 and 6). An additional band (155 nucleotides with probe A, 135 nucleotides with probe B) of variable intensity, even for the same RNA samples, may have arisen from cleavage at an RNase-sensitive site created by the formation of a stable hairpin structure near the 5′ end[4].

In the absence of *tat*, the amount of the full-length HIV-1 LTR transcript was decreased 50-fold (Fig. 4*a*, lanes 3 and 7). We detected several shorter transcripts in these cells (59, 57 and 55 nucleotides with probe A; 39; 37 and 35 nucleotides with probe B) which initiate at position +1 and elongate to positions +55, +57 and +59, respectively. We compared the intensity of the 55–59 nucleotide bands to that of the 205 nucleotide band by densitometer scanning of the autoradiograph in Fig. 4*a*. Whereas in the absence of *tat* ~87% of the correctly initiated transcripts terminated at positions +55 to +59, in the presence of *tat* more than 99% of transcripts were full length. Interestingly, the most prominent transcription endpoint (position +59) corresponds to the junction of two stable RNA stem-loop structures[4]. These structures have a calculated free energy of −37 kcal mole^{-1}, and form under physiological conditions *in vitro*[4]. We conclude that *tat* is required for transcriptional elongation beyond position +59 of the HIV-1 TAR element.

Previously, we demonstrated that *trans*-activation by *tat* increases the steady-state levels of HIV-1 mRNA (ref. 3). Here, we extend these findings by showing that in the absence of *tat*, transcripts that initiate at the HIV-1 cap site end within TAR

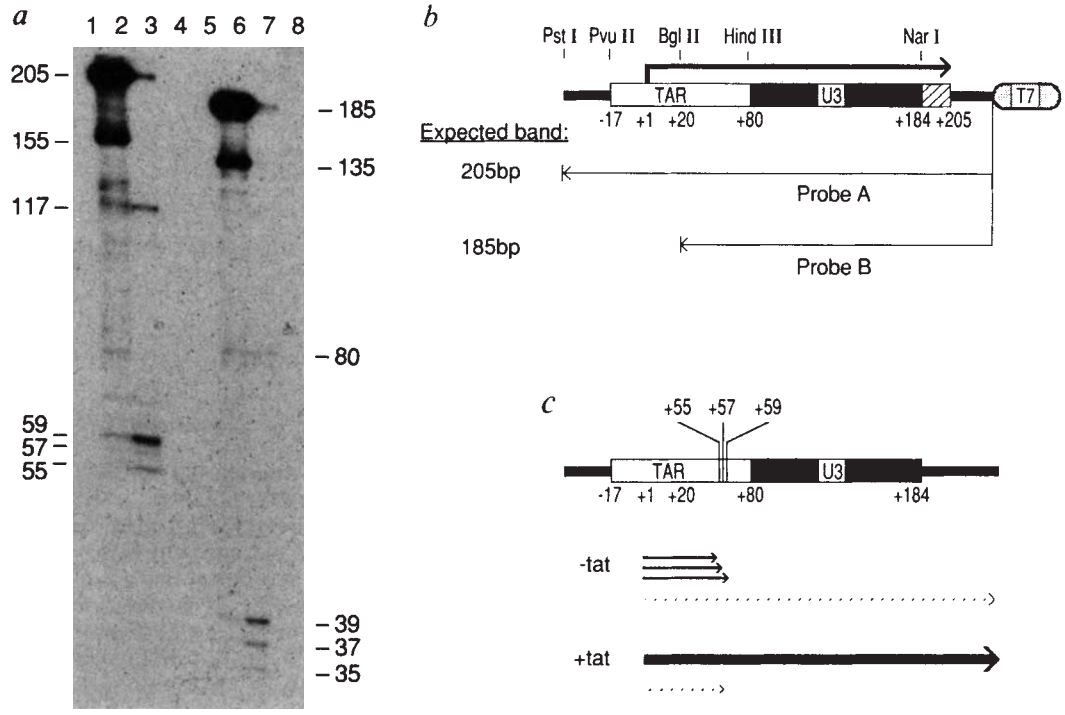

Fig. 4 Mapping of HIV-1 LTR transcripts in co-transfected COS7 cells. *a*, RNase protection assay. Lanes 1 and 5, no RNA; lanes 2 and 6, COS7 cells cotransfected with pHIVCATSV2 and pSVTAT; lanes 3 and 7, COS7 cells cotransfected with pHIVCATSV2 and pSVΔTAT; lanes 4 and 8, untransfected COS7 cells. Lanes 1–4, hybridization to probe A; lanes 5–8, hybridization to probe B (see Fig. 4*b*). Lengths of the hybridizing bands are indicated. The full-length transcripts (205 nucleotides with probe A, 185 nucleotides with probe B) and prematurely terminated transcripts (55–59 nucleotides with probe A, 35–39 nucleotides with probe B) are described in the text. An additional faint band (117 nucleotides with probe A, 80 nucleotides with probe B) was sometimes observed both in the presence and absence of *tat*. These bands may represent transcripts which initiate upstream of the cap site and terminate around position +100, near the polyadenylation site (position +97) of the HIV-1 LTR (ref. 29). They may have escaped detection in the nuclear run-on experiments due to their low abundance. *b*, Antisense RNA probes. Probes A and B were synthesized with bacteriophage T7 RNA polymerase from plasmid pLG1 linearized with *Pst*I or *Bgl*II, respectively. pLG1 contains HIV-1 LTR sequences from positions −17 to +184 cloned into the plasmid vector pGEM-1 (Promega Biotec). Open box, TAR sequences; solid box, HIV-1 LTR U5 sequences; hatched box, polylinker sequences shared between pHIVCATSV2 and pLG1; heavy lines, unshared polylinker sequences; shaded oval, bacteriophage T7 promoter. The arrow above the map indicates the initiation site and direction of HIV-1 LTR transcription. Arrows below the map show the extent of sequences contained within antisense RNA probes A and B. *c*, Diagram of HIV-1 LTR transcripts in the presence and absence of *tat*. The map shows the structure of the TAR and U5 regions. Sites of transcriptional termination at positions +55, +57 and +59 are indicated. Arrows below map show the length of HIV-1 LTR transcripts synthesized in the absence or presence of *tat*. Dotted, thin and thick lines indicate increasing abundance of the transcripts.

Methods. COS7 cells were transfected as in Fig. 2. After 48 h, total cellular RNA was prepared by hot phenol extraction and ethanol precipitation[30]. ^{32}P-labelled RNA probes were synthesized from plasmid pLG1 using α-^{32}P-UTP and bacteriophage T7 RNA polymerase and gel-purified as previously described[3]. Hybridization was carried out as described[3], except that hybridizations contained 10^5 c.p.m. of probe and 5 μg total cellular RNA in a volume of 15 μl. Following hybridization, 75 μl RNase digestion buffer (10 μg ml^{-1} RNase A, 1,300 units ml^{-1} RNase T1, 10 mM Tris-HCl, *p*H 7.5, 300 mM NaCl, 5 mM EDTA) were added and samples were incubated for 1 h at 22 °C. RNases were then inactivated by proteinase K digestion and the ethanol-precipitated RNA samples were analysed by electrophoresis on an 11% polyacrylamide sequencing gel. After autoradiography, the relative molar quantities of the various RNA species were quantified by scanning densitometry. Results were corrected for the length of each hybridizing species as ^{32}P incorporation is proportional to probe length. Identical results were obtained when pHIVCATSV and pSVTATZX were used in place of pHIVCATSV2 and pSVΔTAT, respectively.

between positions +55 and +59. Because these transcripts accumulate in the cytoplasm (M. J. Selby and B.M.P., data not shown), they cannot arise simply from pausing of RNA polymerase, but must result from termination of transcription. We cannot formally exclude the possibility that transcription continues through position +59 in the absence of *tat*, and that the short transcripts arise from cleavage of the primary transcript and subsequent degradation of the 3′ sequences. But such degradation would have to be extremely rapid, because little or no hybridization to CAT sequences was observed with nascent transcripts synthesised in a 5 or 15 minute transcription reaction in the absence of *tat* (Fig. 3*b*). Thus, *tat* acts as a transcriptional anti-terminator. This conclusion is supported by the fact that HIV-1 TAR, like the target sequences of prokaryotic anti-terminators, functions only when positioned in its native orientation, downstream of the site of transcriptional initiation[3,4,15,16].

In a variety of cells the effect of *tat* on the amount of steady-state HIV-1 mRNA can account for *trans*-activation[2–4]. An effect of *tat* on translation of HIV-1 mRNA has also been proposed[5–8]. In COS7 cells, we observed no effect of *tat* upon translation of HIV-1 mRNA as the increases in CAT protein and mRNA levels were equivalent. The run-on transcription experiments suggested that the rate of transcription initiation from the HIV-1 LTR was not affected by *tat*. In the RNase protection assay, however, the total molar quantity of correctly initiated transcripts was about five times lower in the absence of *tat* (by densitometry of gel shown in Fig. 4*a*). This apparent discrepancy could be due to instability of the short transcripts *in vivo*, or to their selective loss during RNA isolation. Also, the length and secondary structure of these RNA species may interfere with hybridization and RNase digestion, leading to underestimation of their abundance. Thus, in the absence of data which directly implicate *tat* in the control of other transcriptional or post-transcriptional events, we conclude that the main and perhaps only function of *tat* in *trans*-activation is to relieve a specific block to transcriptional elongation.

Transcriptional termination and anti-termination are important regulatory mechanisms in many prokaryotic[15–19] and eukaryotic[18–22] genes, including the proto-oncogenes c-*myc* and c-*myb* (refs 23, 24). The study of transcriptional anti-termination in HIV-1 has the advantage that both the *trans*-acting factor (*tat*) and the *cis*-acting sequence (TAR) are known. Analysis of the mechanism of *trans*-activation by *tat* could also be important to the development of drugs designed to block anti-termination by *tat*.

We thank Kathy Jones, Suzanne Mansour, Mark Selby,

Charles Steinberg, Harold Varmus, Matthias Wabl and Michael Walker for discussions and helpful suggestions, Karen Shaw for technical assistance and Michael Armanini for preparation of the manuscript. This work was supported in part by grants from the State of California University wide Task Force on AIDS to BMP and PAL.

Received 2 September; accepted 22 October 1987.

1. Chen, I. S. Y. *Cell* **47**, 1-2 (1986).
2. Rosen, C. A., Sodroski, J. G. & Haseltine, W. A. *Cell* **41**, 813-823 (1985).
3. Peterlin, B. M., Luciw, P. A., Barr, P. J. & Walker, M. D. *Proc. natn. Acad. Sci. U.S.A.* **83**, 9734-9738 (1986).
4. Muesing, M. A., Smith, D. H. & Capon, D. J. *Cell* **48**, 691-701 (1987).
5. Cullen, B. *Cell* **46**, 973-982 (1986).
6. Wright, C. M., Felber, B. K., Paskalis, H. & Pavlakis, G. N. *Science* **234**, 988-992 (1986).
7. Rosen, C. A. *et al. Nature* **319**, 555-559 (1986).
8. Feinberg, M. B., Jarrett, R. F., Aldovini, A., Gallo, R. C. & Wong-Staal, F. *Cell* **46**, 807-817 (1986).
9. Sodroski, J. G. *et al. Science* **229**, 171-173 (1985).
10. Arya, S., Guo, C., Josephs, S. & Wong-Staal, F. *Science* **229**, 69-73 (1985).
11. Sodroski, J. G., Patarca, R., Rosen, C. A., Wong-Staal, F. & Haseltine, W. A. *Science* **229**, 74-77 (1985).
12. Dayton, A., Sodroski, J. G., Rosen, C. A., Goh, W. C. & Haseltine, W. A. *Cell* **44**, 941-947 (1986).
13. Gluzman, Y. *Cell* **23**, 175-182 (1981).
14. Mansour, S. L., Grodzicker, T. & Tjian, R. *Molec. cell. Biol.* **6**, 2684-2694 (1986).
15. Barik, S., Ghosh, B., Whalen, W., Lazinski, D. & Das, A. *Cell* **50**, 885-899 (1987).
16. Grayhack, E. J., Yang, Y., lau, L. F. & Roberts, J. W. *Cell* **42**, 259-269 (1985).
17. Yanofsky, C. *Nature* **289**, 751-758 (1981).
18. Von Hippel, P. H., Bear, D. H., Morgan, W. D. & McSwiggen, J. A. *A. Rev. Biochem.* **53**, 389-446 (1984).
19. Platt, T. *A. Rev. Biochem.* **55**, 339-372 (1986).
20. Dedrick, R. L., Kane, C. M. & Chamberlin, M. J. *J. biol. Chem.* **262**, 9098-9108 (1987).
21. Reines, D., Wells, D., Chamberlin, M. J. & Kane, C. M. *J. molec. Biol.* **196**, 299-312 (1987).
22. Cecli, G., Guise, J. W., McDevitt, M. A., Tucker, P. W. & Nevins, J. R. *Genes Dev.* **1**, 471-481 (1987).
23. Bentley, D. L. & Groudine, M. *Nature* **321**, 702-706 (1986).
24. Bender, T. P., Thompson, C. B. & Kuehl, W. M. *Science* **237**, 1473-1476 (1987).
25. Rio, D. C. & Tjian, R. *Cell* **32**, 1227-1240 (1983).
26. Lusky, M. & Botchan, M. *Nature* **293**, 79-81 (1981).
27. Chirgwin, J. M., Przybyla, A. E., MacDonald, R. J. & Rutter, W. J. *Biochemistry* **18**, 3294-3299 (1979).
28. Church, G. M. & Gilbert, W. *Proc. natn. Acad. Sci. U.S.A.* **81**, 1991-1995 (1984).
29. Sanchez-Pescador, R. *et al. Science* **227**, 484-492 (1985).
30. Queen, C. & Stafford, J. *J. molec. Biol.* **4**, 1042-1049 (1984).

Ultrasound backscatter microscopy images the internal structure of living tumour spheroids

M. D. Sherar, M. B. Noss & F. S. Foster

Ontario Cancer Institute, 500 Sherbourne Street, Toronto, Ontario M4X 1K9, Canada

Ultrasound microscopes have the potential for imaging structure at depth in thick specimens, yet this is not possible in biological specimens using conventional ultrasound transmission or reflection methods[1–3]. But, subsurfacing imaging is possible with ultrasound if a backscatter (pulse-echo) technique, similar to that used in medical imaging, is used[4]. The central problem of extending backscatter imaging to ultrasound microscopy has been the development of high frequency (>100 MHz) transducers with sufficient bandwidth and sensitivity to detect the low levels of backscatter from biological materials. We recently reported the development of such a transducer[5] which we have now incorporated into a new ultrasound backscatter microscope capable of providing tomographic images at depths of up to 4 mm in biological specimens. Here we present the first ultrasound backscatter micrographs of living biological specimens. The benefits of this technique are demonstrated by its application to imaging the internal structures of living tumour spheroids showing striking contrast between the necrotic core and the viable rim of the spheroid.

We have applied a particular mode of ultrasound backscatter imaging called a C-scan[6] to ultrasound microscopy. The microscope geometry and method of imaging are shown in Fig. 1. An ultrasound pulse, generated by the transducer, is brought to a focus in the specimen. The backscattered ultrasound, detected by the same transducer, is time-gated such that only scatter from the focal plane is accepted. The amplitude of this scatter signal is displayed as a brightness value in the image. A complete image is formed by scanning the specimen in two dimensions. The lateral resolution of the microscope is determined by the product of the average wavelength of the ultrasound pulse and the *f*-number (focal length/diameter) of the transducer. Our transducer is operated at 100 MHz with a wavelength of approximately 15 μm in biological specimens and has an *f*-number of 1.33 giving a theoretical resolution of 19.6 μm. The actual resolution (full width at half maximum) was measured to be 17.5 μm which is in good agreement with the theoretical prediction. The thickness of a tomographic slice is determined by the length of the ultrasound pulse. Our high bandwidth transducer is able to produce pulses which are short enough to give image slice thicknesses down to 28 μm. Further details, particularly on the transducer, are given elsewhere[5].

We have applied the ultrasound backscatter microscope to imaging the internal structure of viable multicellular spheroids; a biological system of well known structure on which the microscope could be tested. Spheroids are clonal aggregates of tumour cells which serve as useful *in vitro* models of tumour microregions and early avascular tumour growth. As a spheroid grows, the central regions become depleted of oxygen and nutrients

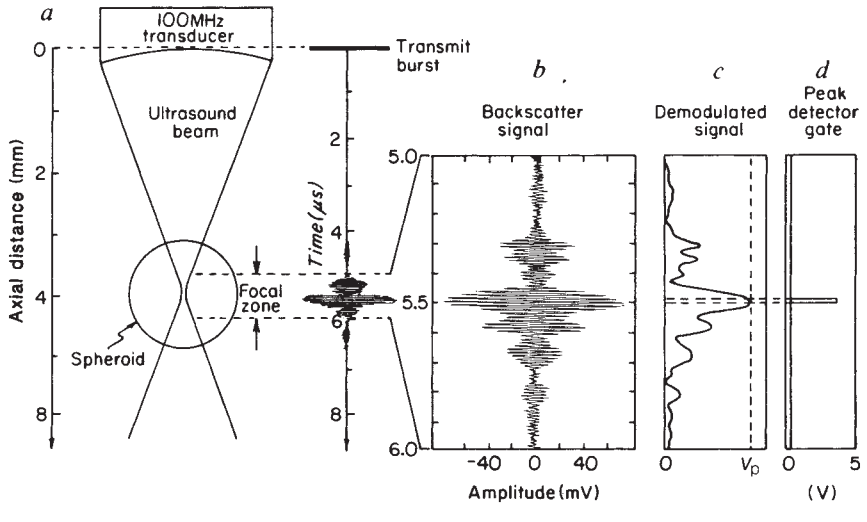

Fig. 1 The ultrasound backscatter microscope and the method of image acquisition. A short, 130 V, 100 MHz electrical burst is transformed by the transducer into a short 100 MHz ultrasound pulse. The pulse is brought to a focus in the specimen (*a*) and the backscattered ultrasound (*b*) is detected at a time corresponding to the depth at which the scattering occurred. Note that the signal amplitude rises to a maximum at a time corresponding to scattering at the transducer focus, where the beam is most intense. This signal is demodulated (*c*) and peak detected in a time window defined by the gate signal (*d*). The peak backscatter signal, V_p, is transferred to a computer and is displayed as a brightness value in the image. A complete image is formed by scanning the ultrasound beam in two dimensions across the plane of interest providing 256×256 measurements, a process which takes approximately 10 min. Planes at different depths are imaged by moving the transducer such that the focus is in the plane of interest and repeating the above process.